WIRELESS COMMUNICATIONS AND MOBILE COMPUTING
Wirel. Commun. Mob. Comput. 2015; **15**:629–638
Published online 2 April 2013 in Wiley Online Library (wileyonlinelibrary.com). DOI: 10.1002/wcm.2371

RESEARCH ARTICLE

A dynamic paging scheme for long-term evolution mobility management

Yi-Bing Lin, Ren-Huang Liou* and Chun-Ting Chang

Department of Computer Science, National Chiao Tung University, Taiwan

ABSTRACT

In *long-term evolution*, the service area is partitioned into several *tracking areas* (TAs), which comprise one or more cells (the radio coverages of base stations). The TAs are grouped into *TA list* (TAL). When an incoming call arrives, the network attempts to connect to the *user equipment* (UE) by paging the cells in the UE's TAL, which may incur large paging traffic that significantly consumes the limited radio resources. To resolve this issue, this paper proposes a *dynamic paging scheme* that determines the paging sequence of cells in real time according to the UE movement and call behavior. We compare the performance of the dynamic paging with that of the previously proposed *Cell-TA-TAL* (CTT) paging. Our study indicates that the dynamic paging outperforms the CTT paging when movement pattern is regular and the UE moves frequently. Copyright © 2013 John Wiley & Sons, Ltd.

KEYWORDS

dynamic paging; long-term evolution (LTE); mobility management

***Correspondence**

Ren-Huang Liou, Department of Computer Science, National Chiao Tung University, Taiwan.
E-mail: rhliou@cs.nctu.edu.tw

1. INTRODUCTION

Mobility management of mobile telecom networks [1–4] tracks the *user equipment* (UE) through the location update and the paging procedures. The location update procedure is executed when the UE moves from one location to another location. When the network attempts to connect to the UE (e.g., when an incoming call arrives), the network executes the paging procedure by broadcasting the paging messages to the base stations where the UE probably resides.

In *long-term evolution* (LTE), the *mobility management entity* (MME; Figure 1 (a)) is responsible for tracking the locations of the UEs [5–7]. The MME is connected to a group of base stations (evolved Node B). The radio coverages of the base stations are called cells (Figure 1 (b)). These cells are grouped into non-overlapped *tracking areas* (TAs) [5,6]. For example, in Figure 1 (c), TA 1 includes Cells 1 and 2. Every TA has a unique *TA identity* (TAI). The TAs are further grouped into the *TA lists* (TALs). The MME allocates the TAL to the UE via the location update procedure. For example, if the UE (Figure 1 (1)) updates its location in Cell 4, the MME allocates TAL 1 (Figure 1 (d)) to the UE, where TAL 1 = {TA 1, TA 2, TA 3}. Every base station periodically broadcasts its TAI. The UE detects that it has left the current TAL by searching the TAL for the TAI received from the the base station. If the received TAI is found in the TAL, it means that the UE does not leave the current TAL. Otherwise, the UE executes the location update procedure to inform the MME of its new location. Then, the MME allocates a new TAL to the UE. In Figure 1, when the UE moves from Cell 4 to Cell 7 (Figure 1 (2)), the received TA 4 identity is not found in TAL 1. Therefore, the UE performs the location update procedure, and the MME allocates TAL 2 to the UE. For the TAL allocation, we consider the *central policy* [5] that allocates the TAL whose central TA is the TA where the UE currently resides. In the central policy, the allocated TALs may be overlapped. For example, in Figure 1, both TALs 1 and 2 include TA 3.

When an incoming call arrives, the MME sends the paging messages to the cells in the UE's TAL to search the UE, which may incur large traffic that significantly consumes the limited radio resources. To resolve this issue, we propose a dynamic paging scheme exercised at the MME to reduce the paging traffic.

This paper is organized as follows. Section 2 proposes the dynamic paging scheme. Section 3 describes a simulation model for this scheme. Section 4 investigates the performance of the dynamic paging scheme by numerical

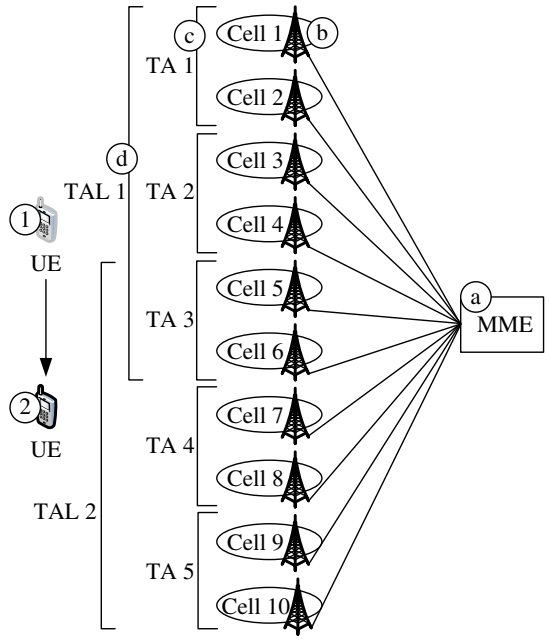

Figure 1. Long-term evolution mobility management architecture.

Table I. The acronym list.

3G	Third-generation
CTT	Cell-TA-TAL
LTE	Long-term evolution
MME	Mobility management entity
TA	Tracking area
TAI	Tracking area identity
TAL	Tracking area list
TT	TA-TAL
UE	User equipment

examples, and the conclusions are given in Section 5. The acronyms used in the paper are listed in Table I.

2. DYNAMIC PAGING SCHEME

On the basis of the TA/TAL architecture described in Section 1, we have considered three paging schemes for LTE mobility management in [8]. The details are reiterated here for the reader's benefit. In these schemes, an *interacted cell* refers to a cell where the UE has interacted with the network (e.g., receives a call or performs a location update).

Scheme Cell-TA-TAL (CTT). When an incoming call arrives, the MME first sends the paging message to the last interacted cell to alert the UE. If the MME does not receive the response within a timeout period, the MME sends the paging messages to the TA of the last interacted cell. If the MME still receives no response from the UE, the MME sends the paging messages to all cells in the TAL.

Scheme TA-TAL (TT). When an incoming call arrives, the MME sends the paging messages to the TA of the last interacted cell. If the MME does not receive the response within a timeout period, the MME sends the paging messages to all cells in the TAL.

Scheme 3G (traditional third-generation approach). When an incoming call arrives, the MME sends the paging messages to all cells in the TAL simultaneously. This scheme is used in the existing 3G mobile networks [1].

We define a *polling cycle* [9] as the period between when the MME sends a paging message to alert the UE and when the MME receives the paging response or a timeout occurs. Let N_p be the maximum number of polling cycles before the UE is found. The numbers N_p of the CTT, the TT, and the 3G schemes are 3, 2, and 1, respectively.

In [8], the performance of the three schemes was evaluated. The study indicated that depending on the UE movement patterns and call activities, one paging scheme may outperform the other two. This paper proposes a dynamic paging scheme that automatically selects the 'best' paging scheme in real time according to the UE movement and call behavior.

Ideally, the dynamic paging selects the paging scheme with the smallest number of paged cells. Practically, the selection decision for a UE is made on the basis of the UE's recent 'behavior history'. Specifically, for the UE, the MME computes the average number of paged cells for the CTT, TT, and 3G schemes in the m most recent incoming call arrivals. When the ith incoming call arrives, we define $C_{p,s}(i)$ as the average number of paged cells for the s scheme in the $m^* = min\{i-1, m\}$ most recent call arrivals, where $s \in \{CTT, TT, 3G\}$. When $i = 1$, we do not have any history datum, and $C_{p,s}(1) = 0$ for all $s \in \{CTT, TT, 3G\}$. To compute $C_{p,s}(i)$ with $i \geq 2$, we first introduce three scenarios when an incoming call arrives. In this paper, we denote N_C and N_T as the number of cells in a TA and the number of TAs in a TAL, respectively.

Scenario 1. The UE resides in the last interacted cell. In this scenario, the number of cells that page the UE for CTT, TT, and 3G schemes are 1, N_C, and $N_C N_T$, respectively. In Figure 1, suppose that the last interacted cell is Cell 4. In this scenario, Cell 4 will page the UE for CTT. On the other hand, Cells 3 and 4 (TA 2) will page the UE for TT, and Cells 1-6 (TAL 1) will page the UE for 3G.

Scenario 2. The UE resides in the TA of the last interacted cell but is not in the last interacted cell. In this scenario, the number of cells that page the UE for CTT, TT, and 3G schemes are $1 + N_C$, N_C, and $N_C N_T$, respectively. In Figure 1, suppose that the last interacted cell is Cell 4. For CTT paging, Cell 4 will page the UE, and then Cells 3 and 4 (TA 2) will page the UE. For TT paging, Cells 3 and 4 (TA 2) will page

the UE. For 3G paging, Cells 1-6 (TAL 1) will page the UE.

Scenario 3. The UE resides in the TAL but is not in the TA of the last interacted cell. In this scenario, the number of cells that page the UE for CTT, TT, and 3G schemes are $1 + N_C + N_C N_T$, $N_C + N_C N_T$ and $N_C N_T$, respectively. In Figure 1, suppose that the last interacted cell is Cell 4. For CTT paging, Cell 4 will page the UE, then Cells 3 and 4 (TA 2) will page the UE, and finally Cells 1–6 (TAL 1) will page the UE. For TT paging, Cells 3 and 4 (TA 2) will page the UE, and then Cells 1–6 (TAL 1) will page the UE. For 3G paging, Cells 1–6 (TAL 1) will page the UE.

In our approach, the MME records the scenario type of each call arrival. Let $n_I(i)$ be the number of scenarios I that occurred between the $(i - m^*)$th call arrival and the $(i-1)$th call arrival where $I \in \{1, 2, 3\}$. On the basis of $n_I(i)$, N_C, and N_T, $C_{p,s}(i)$ is computed as

$$C_{p,CTT}(i) = \begin{cases} \dfrac{n_1(i)}{m^*} + \left\lceil \dfrac{n_3(i)}{m^*} \right\rceil (N_C N_T + 1), & \text{for } N_C = 1 \\ \dfrac{n_1(i)}{m^*} + \left\lceil \dfrac{n_2(i)}{m^*} \right\rceil (1 + N_C) + \left\lceil \dfrac{n_3(i)}{m^*} \right\rceil (1 + N_C + N_C N_T), & \text{for } N_C \neq 1 \end{cases} \quad (1)$$

$$C_{p,TT}(i) = \left\lceil \frac{n_1(i) + n_2(i)}{m^*} \right\rceil N_C + \left\lceil \frac{n_3(i)}{m^*} \right\rceil (N_C + N_C N_T) \quad (2)$$

and

$$C_{p,3G}(i) = N_C N_T \quad (3)$$

In (1), for $N_C = 1$ (i.e., the TA only contains one cell, and scenario 2 never occurs), if the UE is not found in the last interacted cell, all cells in the TAL will page the UE for the CTT paging. Therefore, for the CTT paging with $N_C = 1$, the number of cells that page the UE in scenario 3 is $N_C N_T + 1$. For CTT with $N_C \neq 1$, the numbers of cells that page the UE are 1, $1 + N_C$, and $1 + N_C + N_C N_T$ for scenarios 1, 2, and 3, respectively (as previously mentioned). In (1)–(3), $n_I(i)$ is affected by the movement patterns and call activities of a user. When the ith incoming call arrives, the MME selects the paging scheme with the smallest $C_{p,s}(i)$ among the CTT, TT, and 3G schemes. We note that if two or more schemes have the smallest $C_{p,s}(i)$, the MME selects the one with the smallest N_p to reduce the paging delay.

3. SIMULATION MODEL

This section proposes a discrete-event simulation model (Monte Carlo simulation) to study the performance of the dynamic paging scheme. Note that our previous work indicated that the CTT scheme outperforms both the TT and the 3G schemes with most input parameter setups [8]. Therefore, it suffices to compare the performance of the dynamic paging scheme with that of the CTT scheme. For the dynamic paging (denoted as $s = D$) and the CTT paging (denoted as $s = CTT$), we consider two performance measures as follows:

- $C_{d,s}$: the expected number of polling cycles before the UE is found.
- $C_{p,s}$: the expected number of paged cells when an incoming call arrives.

It is clear that the smaller the aforementioned performance measures, the better the paging scheme.

For the demonstration purpose, we consider a *two-dimensional* (2D) mesh cell configuration (i.e., Manhattan-street-like layout) [10–15]. Figure 2 illustrates the mesh cell configuration, where a cycle represents a cell, and each cell has eight neighboring cells. Various movement patterns can be investigated in our study. To highlight the effect of 'movement locality', we considered the scenario where a UE moves to one direction with a probability different from other directions [15]. In this paper, we extend the previous work by considering the following movement pattern: The UE moves to one of the upper-right, the right, and the lower-right neighboring cells with the routing probability p and moves to one of the other neighboring cells with the probability $(1 - 3p)/5$. It is clear that the movement pattern has the best locality when $p = 0.125$.

On the basis of the mesh cell configuration, Figure 3 shows a TAL configuration, where $N_C = N_T = 9$. In the TAL, the cells are labeled as $\langle x, y \rangle$, where x is the column label, y is the row label, and $1 \leq x, y \leq \sqrt{N_C N_T}$. The

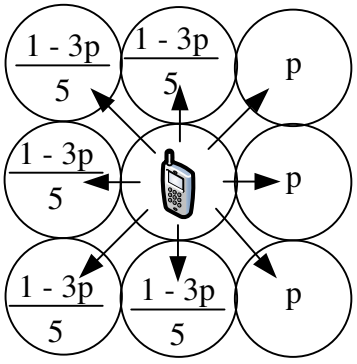

Figure 2. Mesh cell configuration and the movement directions.

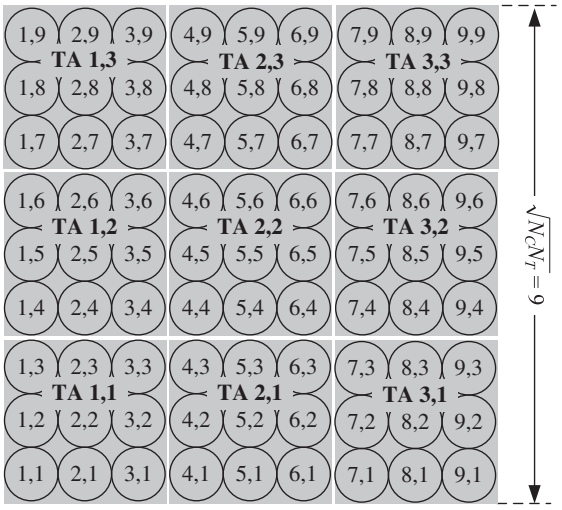

Figure 3. An example of the tracking area (TA) list configuration ($N_C = N_T = 9$).

TAs are labeled as $\langle X, Y \rangle$, where $1 \leq X, Y \leq \sqrt{N_T}$. TA $\langle X, Y \rangle$ consists of cells $\langle x, y \rangle$ where $(X-1)\sqrt{N_C}+1 \leq x \leq X\sqrt{N_C}$ and $(Y-1)\sqrt{N_C}+1 \leq y \leq Y\sqrt{N_C}$. To simplify the discussions on the central policy, we assume that $\sqrt{N_T}$ is an odd number. Because the central policy is exercised, when the UE leaves the current TAL, the entrance TA is reset to the central TA of the 'next' TAL, and the entrance cell is reset to the cell in the central TA at the same relative position. For example, in Figure 3, when the UE in Cell $\langle 9, 1 \rangle$ moves to the right-hand side neighboring cell, the entrance cell is reset to Cell $\langle 4, 4 \rangle$. In the simulation, an event e has two attributes as follows:

- The $type$ attribute indicates one of the two event types. A **Call** event represents a call arrival. When the **Call** event occurs, the MME searches the UE through the paging procedure. A **Move** event represents that the UE crosses the cell boundary to a neighboring cell.
- The ts attribute indicates the timestamp when the event occurs.

The inter-call arrival time t_c is a random number drawn from an exponential generator G_C with the mean $1/\lambda_c$. The residence time t_m that the UE stays in a cell is a random number drawn from a Gamma generator G_M with the mean $1/\lambda_m$ and the variance V. We consider the Gamma distribution because this distribution is widely used in telecom modeling [8,9,15–18]. Other distributions such as Weibull and truncated Normal show similar results and will not be presented here. Let U be a uniform random number between 0 and 1 drawn from a generator G_D. In this simulation, the last interacted cell is labeled as $\langle \bar{x}, \bar{y} \rangle$, and the cell where the UE currently resides is represented by $\langle x^*, y^* \rangle$. Three counters are used to measure the output statistics as follows:

- i: the number of incoming calls.
- n_d: the number of polling cycles.
- n_p: the number of paged cells.

From the aforementioned counters, we compute

$$C_{d,s} = \frac{n_d}{i} \text{ and } C_{p,s} = \frac{n_p}{i} \tag{4}$$

The details of the simulation procedure are given in Appendix A.

We validate the simulation model of the dynamic paging by two analytic models as follows. Our previous work [8] proposed the analytic models to derive the paging costs of the CTT and TT schemes for the *one-dimensional* (1D) TAL configuration. The validation procedure is described with the following steps:

Step 1.1. For some input parameter setups (e.g., $\lambda_m/\lambda_c = 0.01$, $V = 1/\lambda_m^2$, $N_C = 3$, $N_T = 15$, $p = 0.5$, and $m = 50$), the dynamic paging will select the CTT scheme to search the UE in most incoming calls (more than 99%). In this case, we compare the paging cost of the dynamic paging with that of the CTT scheme derived in [8]. Our study indicates that the analytic and simulation results are consistent (the discrepancies are within 1%), and the details are omitted.

Step 1.2. Similar to Step 1.1, when $\lambda_m/\lambda_c = 10$, $V = 1/\lambda_m^2$, $N_C = 3$, $N_T = 15$, $p = 0.9$, and $m = 50$, the dynamic paging will select the TT scheme in most incoming calls. Our study also shows that the analytic and simulation results are consistent (the discrepancies are within 1%).

Step 1.3. For other input parameter setups, the dynamic paging may not always select the same paging scheme. We modify the simulation program to record the percentages of calls where the CTT, TT, and 3G schemes are exercised. From the percentages and the paging costs derived in [8], we compute the expected paging cost of the dynamic paging scheme and compare the expected paging cost with the simulation results. Our study indicates that the discrepancies are within 1%, and the analytic analysis is consistent with the simulation results.

4. NUMERICAL EXAMPLES

This section compares the performance of the dynamic paging scheme and the CTT paging scheme by numerical examples. We consider the TAL's size $N_C N_T = 15^2$. For other $N_C N_T$ values, the results are similar and are omitted. Our simulation experiments also show that $m \geq 10$ is appropriate. In this paper, we consider $m = 20$ and $N_C = 3^2$.

4.1. Analysis of the $C_{d,s}$ performance

This subsection investigates the effects of p, λ_m/λ_c, and V on the expected number $C_{d,s}$ of polling cycles before the UE is found.

Effects of p: When p increases, the UE tends to move to the right-hand side neighboring cells, and worse locality is expected. In this case, the UE is more likely to be far away from the last interacted cell. Therefore, both $C_{d,D}$ and $C_{d,CTT}$ increase as p increases. Figure 4 (a) shows that $C_{d,D}/C_{d,CTT}$ increases as p increases, and the effect of p becomes more significant when λ_m/λ_c increases (to be discussed next). Clearly, the more the locality, the more the dynamic scheme outperforms the CTT scheme.

Effects of λ_m/λ_c: When λ_m/λ_c increases (i.e., more cell crossings during t_c), the UE may be far away from the last interacted cells, and higher $C_{d,D}$ and $C_{d,CTT}$ are expected. Figure 4 (b) indicates that $C_{d,D}/C_{d,CTT}$ decreases as λ_m/λ_c increases. This phenomenon is explained as follows. When λ_m/λ_c increases, the dynamic paging is more likely to select the TT or the 3G scheme because the UE may be far away from the last interacted cell. Because the paging delays of the TT and 3G schemes are smaller than that of the CTT scheme, $C_{d,D}/C_{d,CTT}$ decreases as λ_m/λ_c increases. The figure shows that the dynamic

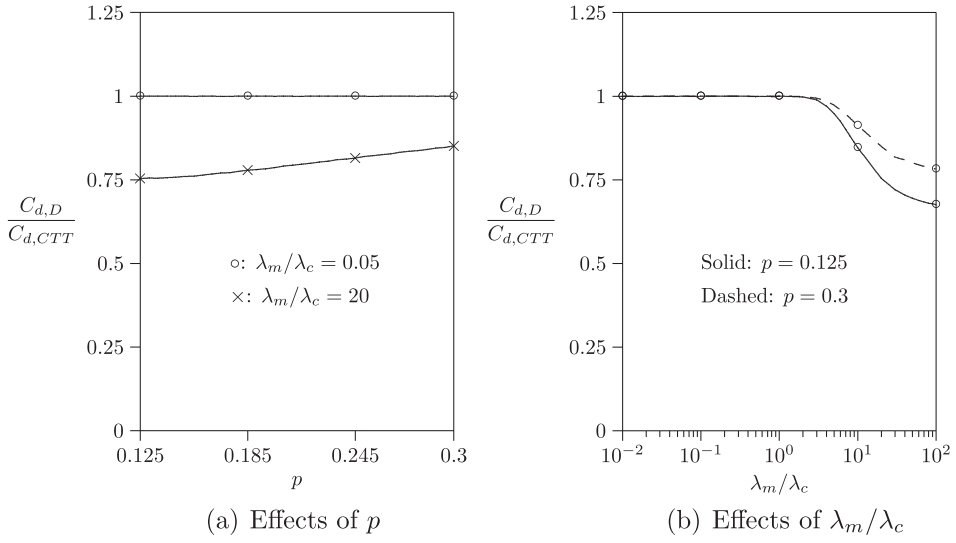

Figure 4. Effects of p and λ_m/λ_c on $C_{d,D}/C_{d,CTT}$ ($N_C = 3^2$, $N_T = 5^2$, $m = 20$, and $V = 1/\lambda_m^2$).

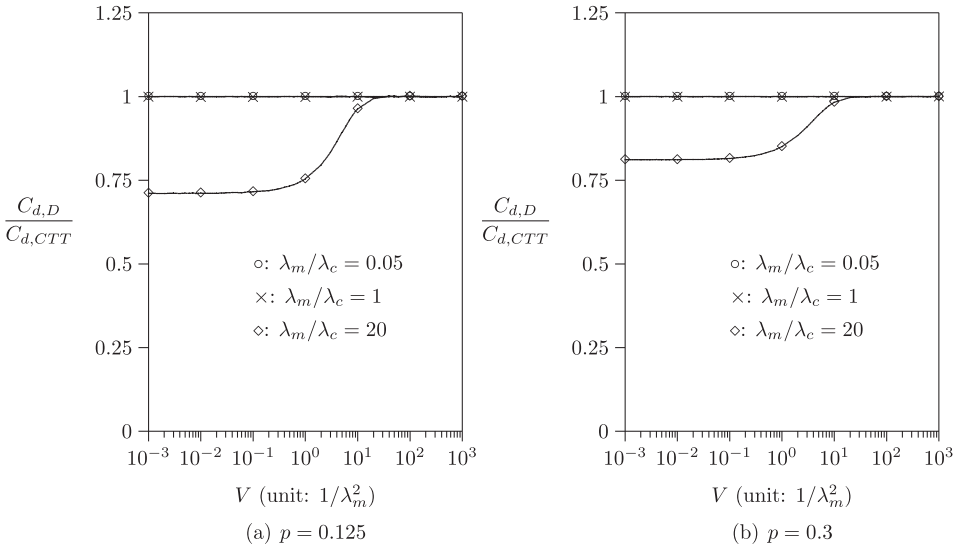

Figure 5. Effects of V and p on $C_{d,D}/C_{d,CTT}$ ($N_C = 3^2$, $N_T = 5^2$, and $m = 20$).

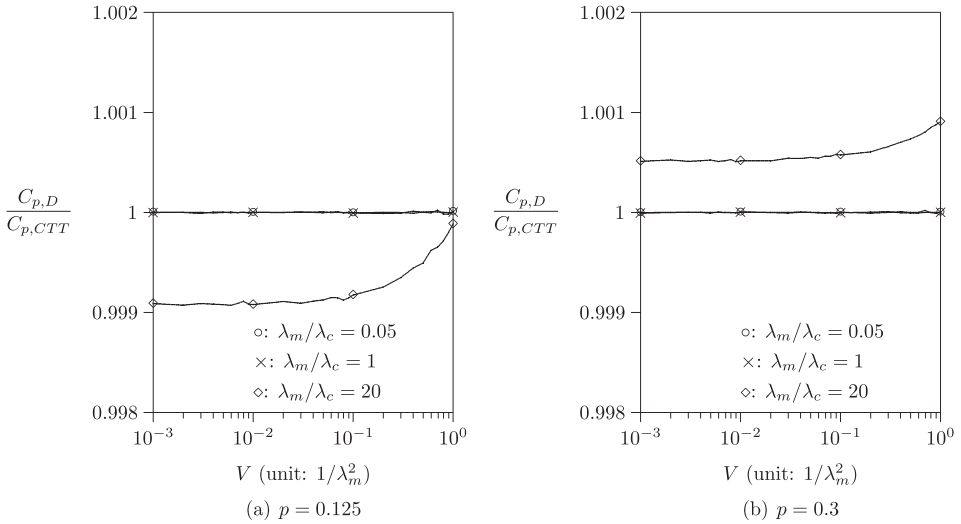

Figure 6. Effects of λ_m/λ_c, p, and V on $C_{p,D}/C_{p,CTT}$ ($N_C = 3^2$, $N_T = 5^2$, and $m = 20$).

scheme outperforms the CTT scheme in the λ_m/λ_c range being considered. We have also considered the scenario where λ_m/λ_c changes from time to time, and similar results are observed, which will not be presented here.

Effects of V: When V is small (i.e., movement pattern is regular), most t_m values are close to $1/\lambda_m$. In this case, if λ_m/λ_c is small, the UE is more likely to be found in the last interacted cell, and the dynamic and CTT schemes have similar (and good) $C_{d,s}$ performance (in Figure 5, for $V \leq 1/\lambda_m^2$, the values of the $\circ$ and $\times$ curves are close to 1). On the other hand, when λ_m/λ_c is large, dynamic paging outperforms CTT paging because the dynamic paging scheme is more likely to select the TT or the 3G scheme, which has smaller paging delay (in Figure 5, for $V \leq 1/\lambda_m^2$, the values of the $\diamond$ curves are smaller than 1). For any λ_m value, when V increases, more longer t_m periods are observed, and the UE does not move in many consecutive t_c periods that fall in these t_m. In this case, the UE is always found in the last interacted cell, and both the dynamic paging and the CTT paging have similar performance (in Figures 5, for $V > 10^2/\lambda_m^2$, the values of all curves are close to 1).

4.2. Analysis of the $C_{p,s}$ performance

This subsection investigates the expected number $C_{p,s}$ of paged cells when an incoming call arrives. The effects of λ_m/λ_c, p, and V on $C_{p,s}$ are similar to those on $C_{d,s}$ described in Subsection 4.1. However the 'degrees' of the effects of these parameters on $C_{p,s}$ and $C_{d,s}$ for the CTT and the dynamic schemes are different. A nontrivial result is that $C_{p,D}/C_{p,CTT} \approx 1$ for various λ_m/λ_c, p, and V values (as illustrated in Figure 6). The reason is given as follows. When λ_m/λ_c is small, it is more likely to find the UE in the last interacted cell. In this case, dynamic paging selects the CTT scheme to search the UE, and both the dynamic and CTT pagings have similar and good performance (in Figure 6, the values of the $\circ$ and $\times$ curves are close to 1). On the other hand, when λ_m/λ_c is large, the dynamic paging is more likely to select the TT or the 3G scheme. In this case, if p is small, we observe that the dynamic paging likely selects the TT scheme, which has a slightly lower paging cost than the CTT scheme [8]. Therefore, the dynamic paging outperforms the CTT paging (in Figure 6(a), the values of the $\diamond$ curve are smaller than 1). On the other hand, if p is large, because of the high paging cost of the 3G scheme, the paging cost of the dynamic scheme is slightly higher than that of the CTT scheme (in Figure 6(b), the values of the $\diamond$ curve are slightly larger than 1). We note that the performance discrepancies of the paging cost between the dynamic and the CTT pagings are within 0.2% for all input parameter setups under our study.

5. CONCLUSIONS

This paper proposed the dynamic paging scheme for LTE mobility management. The performance is measured by the expected number $C_{d,s}$ of polling cycles before the UE is found and the expected number $C_{p,s}$ of paged cells when an incoming call arrives. We compare the performance of the dynamic paging with the best static paging scheme called CTT. Our study indicates the following results:

- For the $C_{d,s}$ performance, when V is small and λ_m/λ_c is large (i.e., movement pattern is regular and the UE moves frequently), the dynamic paging outperforms the CTT paging. On the other hand, when V is large or λ_m/λ_c is small, the

dynamic paging and the CTT paging have similar performance.
- For the $C_{p,s}$ performance, the dynamic and CTT schemes have similar performance for all input parameter setups under our study.

In summary, the dynamic paging scheme is better than the CTT paging scheme.

APPENDIX A: DETAILED SIMULATION PROCEDURES

This appendix describes the detailed simulation procedures for the dynamic and CTT schemes. A clock t is maintained to indicate the simulation progress, which is the timestamp of the event being processed. All events are inserted into the event list and are deleted/processed from the event list in the non-decreasing timestamp order. An array $I[i]$ is maintained to record the scenario type of the ith incoming call (e.g., $I[i] = 1$ means that the UE resides in the last interacted cell when the ith call arrives). Figure A.1 illustrates the simulation flow chart for the dynamic paging scheme with the following steps:

Step 1. Set the counters (i.e., i, n_d, and n_p) and the simulation clock t to 0. Initialize $\bar{x}$, $\bar{y}$, x^*, and y^* by randomly selecting integers from 1 to $\sqrt{N_C N_T}$.

Step 2. The first **Call** event e_1 and **Move** event e_2 are generated. For event e_1, $e_1.type$ is **Call**, and $e_1.ts = t + t_c$ where t_c is generated from G_C. For event e_2, $e_2.type$ is **Move**, and $e_2.ts = t + t_m$ where t_m is generated from G_M. Events e_1 and e_2 are inserted into the event list.

Steps 3 and 4. The first event e in the event list is deleted and processed on the basis of its type. The simulation clock t is set to $e.ts$. If $e.type$ is **Call**, Step 5 is executed. If $e.type$ is **Move**, the simulation proceeds to Step 20.

Steps 5–17 simulate a **Call** event, which are described as follows.

Step 5. When an incoming call arrives, i is incremented by one.

Step 6. As mentioned in Section 2, if $i = 1$, we do not have any history datum to estimate the paging cost of each paging scheme. In this case, we select the 3G scheme because the 3G scheme has the smallest paging delay, and Step 15 is executed. Otherwise, the flow goes to Step 7.

Step 7. The MME computes $n_I(i)$ based on $I[j]$ where $i - m^* \le j \le i - 1$, and for $s \in \{CTT, TT, 3G\}$, $C_{p,s}(i)$ are calculated from $n_I(i)$ and equations (1)–(3).

Step 8. As mentioned in Section 2, the MME selects the paging scheme s with the smallest $C_{p,s}(i)$. If two or more schemes have the smallest $C_{p,s}(i)$, the one with the smallest N_p is selected.

Step 9. If $s = CTT$, Step 10 is executed. If $s = TT$, the simulation proceeds to Step 13. If $s = 3G$, the flow goes to Step 15.

Steps 10 and 11 (CTT is exercised). The MME sends the paging message to the last interacted cell, and both n_d and n_p are incremented by one. If the UE resides in the last interacted cell (i.e., $x^* = \bar{x}$ and $y^* = \bar{y}$), then the UE will receive the paging message, and the simulation proceeds to Step 16. Otherwise, Step 12 is executed.

Step 12. If a TA only contains one cell (i.e., $N_C = 1$), the TA of the last interacted cell has paged the UE in Step 10, and the UE is not found in Step 11. In this case, Step 15 is executed to search the UE in all cells of the TAL. Otherwise, the flow goes to Step 13.

Steps 13 and 14 (TT is exercised). The MME sends the paging messages to the TA of the last interacted cell. Therefore, n_p is incremented by N_C, and n_d is incremented by one. If the UE resides in the TA of the last interacted cell (i.e., $\lceil x^*/\sqrt{N_C} \rceil = \lceil \bar{x}/\sqrt{N_C} \rceil$ and $\lceil y^*/\sqrt{N_C} \rceil = \lceil \bar{y}/\sqrt{N_C} \rceil$), the UE is found, and Step 16 is executed. Otherwise, the simulation proceeds to Step 15.

Step 15 (3G paging is exercised). The MME sends the paging messages to all cells in the TAL. Therefore, n_p is incremented by $N_C N_T$, and n_d is incremented by one.

Step 16. The MME records the scenario type $I[i]$ of the ith incoming call as follows:

if $x^* = \bar{x}$ and $y^* = \bar{y}$ **then** $I[i] \leftarrow 1$;
else if $\lceil x^*/\sqrt{N_C} \rceil = \lceil \bar{x}/\sqrt{N_C} \rceil$ and $\lceil y^*/\sqrt{N_C} \rceil = \lceil \bar{y}/\sqrt{N_C} \rceil$ **then** $I[i] \leftarrow 2$;
else $I[i] \leftarrow 3$.

Then, the MME updates the last interacted cell by setting $\langle \bar{x}, \bar{y} \rangle$ to $\langle x^*, y^* \rangle$.

Step 17. The next **Call** event e_1 is generated and inserted into the event list, where $e_1.ts = t + t_c$.

Step 18. If 10 million of **Call** events have been processed, Step 19 is executed. Otherwise, Step 3 is executed. In our experience, 10 million of **Call** events are enough to produce stable statistics.

Step 19. The performance measures are computed by (4), and the simulation terminates.

Steps 20–24 handle a **Move** event, which are described as follows.

Step 20. When the UE crosses the cell boundary to a neighboring cell, the movement direction is determined by the uniform random number U generated by G_D. From Figure 2, new $\langle x^*, y^* \rangle$ are updated by the following routing rules:

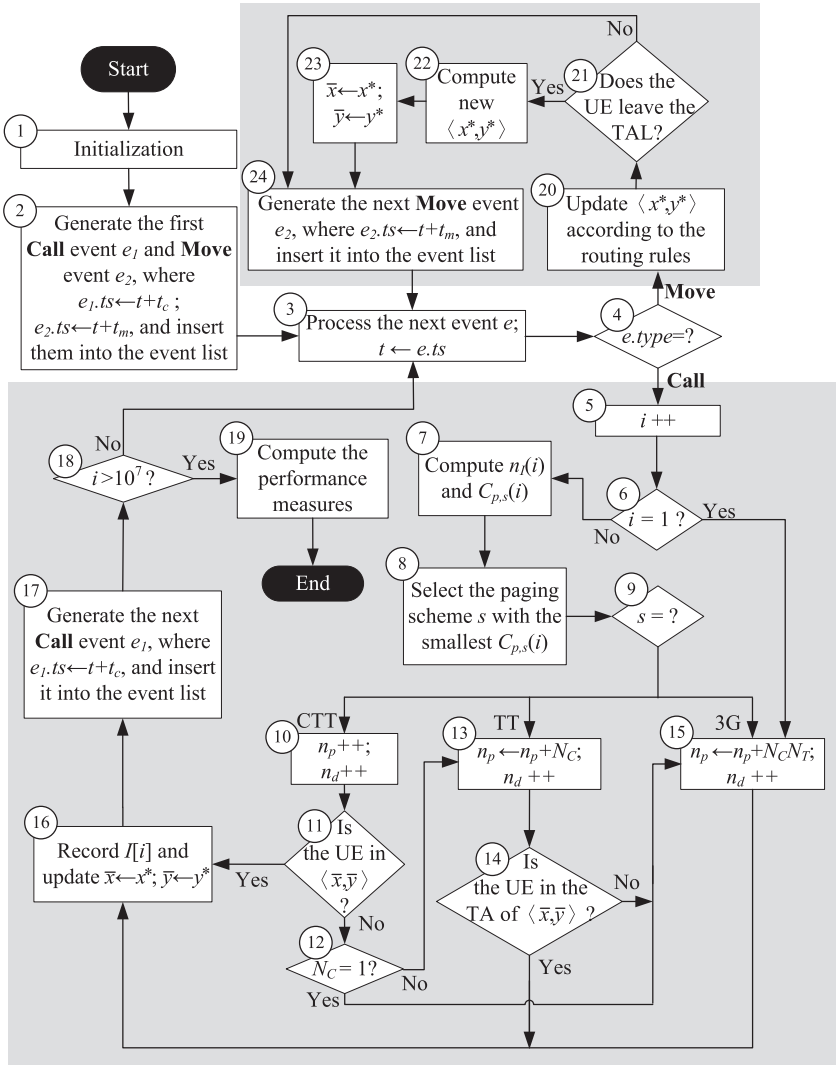

Figure A.1. Simulation flow chart for the dynamic paging scheme.

$$\langle x^*, y^* \rangle \leftarrow \begin{cases} \langle x^*-1, y^*+1 \rangle, & \text{for } 0 \le U < \dfrac{1-3p}{5} \\ \langle x^*-1, y^* \rangle, & \text{for } \dfrac{1-3p}{5} \le U < \dfrac{2(1-3p)}{5} \\ \langle x^*-1, y^*-1 \rangle, & \text{for } \dfrac{2(1-3p)}{5} \le U < \dfrac{3(1-3p)}{5} \\ \langle x^*, y^*+1 \rangle, & \text{for } \dfrac{3(1-3p)}{5} \le U < \dfrac{4(1-3p)}{5} \\ \langle x^*, y^*-1 \rangle, & \text{for } \dfrac{4(1-3p)}{5} \le U < 1-3p \\ \langle x^*+1, y^*+1 \rangle, & \text{for } 1-3p \le U < 1-2p \\ \langle x^*+1, y^* \rangle, & \text{for } 1-2p \le U < 1-p \\ \langle x^*+1, y^*-1 \rangle, & \text{for } 1-p \le U \le 1 \end{cases} \tag{A.1}$$

Step 21. If the UE leaves the current TAL (i.e., $x^* = 0$ or $\sqrt{N_C N_T} + 1$, or $y^* = 0$ or $\sqrt{N_C N_T} + 1$), Step 22 is executed. Otherwise, Step 24 is executed.

Step 22. As mentioned before, when the UE leaves the current TAL, the entrance cell is reset to the cell in the central TA. Therefore, x^* and y^* are set as

$$x^* \leftarrow \sqrt{N_C}\left(\left\lceil \frac{\sqrt{N_T}}{2} \right\rceil - \left\lceil \frac{x^*}{\sqrt{N_C}} \right\rceil\right) + x^* \quad \text{(A.2)}$$

and

$$y^* \leftarrow \sqrt{N_C}\left(\left\lceil \frac{\sqrt{N_T}}{2} \right\rceil - \left\lceil \frac{y^*}{\sqrt{N_C}} \right\rceil\right) + y^* \quad \text{(A.3)}$$

Step 23. The MME updates the last interacted cell by setting $\langle \bar{x}, \bar{y} \rangle$ to $\langle x^*, y^* \rangle$.

Step 24. The next **Move** event e_2 is generated and inserted into the event list, where $e_2.ts = t + t_m$. The simulation jumps to Step 3.

The simulation flow chart for the CTT scheme is similar to that in Figure A.1 except that Steps 6–9 and the array $I[i]$ in Step 16 are not needed in the CTT simulation. Moreover, after the execution of Step 5, the CTT simulation goes to Step 10.

APPENDIX B: NOTATION

The notation used in this paper is listed in the succeeding text.

- p: the probability that the UE moves to one of the upper-right, right, and lower-right neighboring cells.
- $\langle x, y \rangle$: the label of an arbitrary cell in a TAL (x: column label; y: row label).
- $\langle \bar{x}, \bar{y} \rangle$: the label of the last interacted cell ($\bar{x}$: column label; $\bar{y}$: row label).
- $\langle x^*, y^* \rangle$: the label of the cell where the UE currently resides (x^*: column label; y^*: row label).
- $\langle X, Y \rangle$: the label of an arbitrary TA in a TAL (X: column label; Y: row label).
- $C_{d,s}$: the expected number of polling cycles before the UE is found for the dynamic paging ($s = D$) and the CTT paging ($s = CTT$), respectively.
- $C_{p,s}$: the expected number of paged cells when an incoming call arrives for the dynamic paging ($s = D$) and the CTT paging ($s = CTT$), respectively.
- $C_{p,s}(i)$: the average number of paged cells for the s scheme between the $(i - m^*)$th call arrival and the $(i - 1)$th call arrival, where $s \in \{CTT, TT, 3G\}$.
- t: the simulation clock.
- t_c: the inter-call arrival time.
- t_m: the cell residence time.
- $1/\lambda_c = E[t_c]$: the mean inter-call arrival time.
- $1/\lambda_m = E[t_m]$: the mean cell residence time.
- V: the variance for the t_m distribution.
- m: the number of the most recent incoming call arrivals.
- m^*: the smaller of $i - 1$ and m.
- N_C: the number of cells in a TA.
- N_T: the number of TAs in a TAL.
- N_p: the maximum number of polling cycles before the UE is found.
- $n_I(i)$: the number of scenarios I occurred between the $(i - m^*)$th call arrival and the $(i - 1)$th call arrival where $I \in \{1, 2, 3\}$.
- i: the number of incoming calls.
- n_d: the number of polling cycles.
- n_p: the number of paged cells.
- G_C: the exponential random number generator.
- G_M: the Gamma random number generator.
- G_D: the uniform random number generator.
- e, e_1, e_2: the events in the simulation.
- U: the uniform random number drawn from G_D.
- $I[i]$: the scenario type of the ith incoming call arrival.
- s: the paging scheme ($s = D$ for dynamic paging, $s = CTT$ for Cell-TA-TAL paging, $s = TT$ for TA-TAL paging, and $s = 3G$ for third generation paging).

ACKNOWLEDGEMENTS

Y.-B. Lin's work was supported in part by the NSC 100-2221-E-009-070 and 101-2221-E-009-032, Academia Sinica AS-102-TP-A06, Chunghwa Telecom, IBM, Arcadyan Technology Corporation, the ITRI/NCTU JRC Research Project, the ICL/ITRI Project, Nokia Siemens Networks, Department of Industrial Technology (DoIT) Academic Technology Development Program 100-EC-17-A-03-S1-193, and the MoE ATU plan. R.-H. Liou's work was supported by the MediaTek Fellowship.

REFERENCES

1. Lin Y-B, Pang A-C. *Wireless and Mobile All-IP Networks*. John Wiley & Sons, Inc.: Indianapolis, Indiana, 2005.
2. Pan Y-N, Chen W-E. Enhanced secure SIP/IMS mobility in integrated UMTS-WLAN networks, In *Smart Mobility*, Nice, France, 2011.
3. Yang S-R, Lin Y-B. Performance evaluation of location management in UMTS. *IEEE Transactions on Vehicular Technology* 2003; **52**(6): 1603–1615.
4. Lin Y-B, Pang A-C, Rao Herman C-H. Impact of mobility on mobile telecommunications networks. *Wireless Communications and Mobile Computing* 2005; **5**(7): 713–732.
5. 3rd Generation Partnership Project; Technical Specification Group Services and System Aspects; General Packet Radio Service (GPRS) enhancements for

Evolved Universal Terrestrial Radio Access Network (E-UTRAN) access, 3GPP. *Technical Specification 3G TS 23.401 version 10.0.0 (2010-06)*, 2010.
6. 3GPP. 3rd Generation Partnership Project; Technical Specification Group Radio Access Network; Evolved Universal Terrestrial Radio Access (E-UTRA) and Evolved Universal Terrestrial Radio Access Network (E-UTRAN); Overall description; Stage 2. *Technical Specification 3G TS 36.300 version 10.1.0 (2010-09)*, 2010.
7. Punz G. *Evolution of 3G Networks: The Concept, Architecture and Realization of Mobile Networks Beyond UMTS*. Springer: New York, 2010.
8. Liou R-H, Lin Y-B, Tsai S-C. An investigation on LTE mobility management. *IEEE Transactions on Mobile Computing* 2013; **12**(1): 166–176.
9. Akyildiz I, Ho J, Lin Y-B. Movement-based location update and selective paging for PCS networks. *IEEE/ACM Transactions on Networking* 1996; **4**(4): 629–638.
10. Maxemchuk N. Routing in the Manhattan street network. *IEEE Transactions on Communications* 1987; **35**(5): 503–512.
11. Meyer H, Trullols-Cruces O, Hess A, Hummel K, Barcelo-Ordinas J, Casetti C, Karlsson G. VANET mobility modeling challenged by feedback loops, In *2011 the 10th IFIP Annual Mediterranean Ad Hoc Networking Workshop* (Med-Hoc-Net), Sicily, Italy, 2011; 95–102.
12. Kraaier J, Killat U. The influence of user mobility on vehicular internet access via IEEE 802.11 access points, In *IEEE International Conference on Wireless and Mobile Computing, Networking and Communications*, Montreal, Canada, 2006; 335–342.
13. Tchakountio F, Ramanathan R. Tracking highly mobile endpoints, In *Proceedings of the 4th ACM International Workshop on Wireless Mobile Multimedia*, Rome, Italy, 2001; 83–94.
14. Moustafa M, Habib I, Naghshineh M. Efficient radio resource control for Manhattan street environments. *IEEE International Conference on Communications* 2002; **5**: 3377–3381.
15. Liou R-H, Lin Y-B. Mobility management with the central-based location area policy. *Computer Networks* 2012. DOI: 10.1016/j.comnet.2012.11.003.
16. Lai Y-C, Lin P, Cheng S-M. Performance modeling for application-level integration of heterogeneous wireless networks. *IEEE Transactions on Vehicular Technology* 2009; **58**(5): 2426–2434.
17. Sou S-I, Jeng J-Y, Lin P. Improving session continuity through user mobility tracking for EPS interserving gateway handover. *Wireless Communications and Mobile Computing* 2012; **12**(12): 1077–1090.
18. Pang A-C, Chen Y-K. A multicast mechanism for mobile multimedia messaging service. *IEEE Transactions on Vehicular Technology* 2004; **53**(6): 1891–1902.

AUTHORS' BIOGRAPHIES

Yi-Bing Lin is the vice president and life chair professor of the College of Computer Science, National Chiao Tung University (NCTU) and a visiting professor of King Saud University. He is also with the Institute of Information Science and the Research Center for Information Technology Innovation, Academia Sinica, Nankang, Taipei, Taiwan. Lin is the author of the books *Wireless and Mobile Network Architecture* (Wiley, 2001), *Wireless and Mobile All-IP Networks* (John Wiley, 2005), and *Charging for Mobile All-IP Telecommunications* (Wiley, 2008). Lin received numerous research awards including the 2005 NSC Distinguished Researcher and the 2006 Academic Award of Ministry of Education. Lin is a fellow of ACM, AAAS, IEEE, and IET.

Ren-Huang Liou received his BS and MS degrees in Computer Science from the National Chiao Tung University (NCTU), Hsinchu, Taiwan, in 2007 and 2009, respectively. He is currently working toward his PhD degree at NCTU. His current research interests include Voice over Internet Protocol (VoIP), mobile computing, and performance modeling.

Chun-Ting Chang received his BS degree in Computer Science from the National Chiao Tung University (NCTU), Hsinchu, Taiwan, in 2012. She is currently working toward her MS degree at NCTU. Her current research interests include design and analysis of personal communications services network and mobile augmented reality.